

Effect of Film-Hole Shape on Turbine-Blade Heat-Transfer Coefficient Distribution

Shuye Teng* and Je-Chin Han†

Texas A&M University, College Station, Texas 77843-3123

and

Philip E. Poinsatte‡

NASA John H. Glenn Research Center at Lewis Field, Cleveland, Ohio 44135-3191

Detailed heat-transfer coefficient distributions on the suction side of a gas turbine blade were measured using a transient liquid crystal image method. The blade has only one row of film holes near the gill-hole portion on the suction side of the blade. Studies on three different kinds of film-cooling hole shapes were presented. The hole geometries studied include standard cylindrical holes and holes with a diffuser-shaped exit portion (i.e., fan-shaped holes and laidback fan-shaped holes). Tests were performed on a five-blade linear cascade in a low-speed wind tunnel. The mainstream Reynolds number based on the cascade exit velocity was 5.3×10^5 . Upstream unsteady wakes were simulated using a spoke-wheel-type wake generator. The wake Strouhal number was kept at 0 and 0.1. The coolant-to-mainstream blowing ratio was varied from 0.4 to 1.2. The results show that unsteady wake generally tends to induce earlier boundary-layer transition and enhance the surface heat-transfer coefficients. When compared to the cylindrical hole case, both the expanded hole injections have much lower heat-transfer coefficients over the surface downstream of the injection location, particularly at high blowing ratios. However, the expanded hole injections induce earlier boundary-layer transition to turbulence and enhance heat-transfer coefficients at the latter part of the blade suction surface.

Nomenclature

| | |
|------------------|---|
| C_x | = blade axial chord length (17 cm) |
| D | = film-hole diameter |
| d | = wake generator rod diameter |
| h | = local heat-transfer coefficient |
| k | = thermal conductivity of blade material ($0.159 \text{ W/m} \cdot ^\circ\text{C}$) |
| k_{air} | = thermal conductivity of mainstream air |
| L | = film-cooling hole length |
| M | = coolant-to-mainstream mass flux ratio or blowing ratio, $\rho_c V_c / \rho_m V$ |
| N | = speed of rotating rods |
| Nu | = local Nusselt number based on axial chord, $h C_x / k_{\text{air}}$ |
| \bar{Nu} | = spanwise-averaged Nusselt number |
| n | = number of rods on wake generator |
| P | = film-hole pitch |
| Re | = Reynolds number based on exit velocity and axial chord, $V_2 C_x / \nu$ |
| S | = wake Strouhal number, $2\pi N d n / (60 V_1)$ |
| SL | = streamwise length on the suction surface (33.1 cm) |
| T_c | = coolant temperature |
| T_i | = initial temperature of blade surface |
| T_m | = mainstream temperature |
| T_w | = liquid crystal color change from green to red |
| \bar{Tu} | = mean turbulence intensity |
| t | = liquid crystal color change time |
| V_1 | = cascade inlet velocity |
| V_2 | = cascade exit velocity |

| | |
|------------|--|
| X | = streamwise distance starting from film-hole centerline; streamwise distance measured from leading edge to film-hole centerline |
| Y | = perpendicular distance from blade surface |
| α | = thermal diffusivity of blade material ($0.135 \times 10^{-6} \text{ m}^2/\text{s}$) |
| δ_2 | = local momentum thickness |
| ν | = kinematic viscosity of cascade inlet mainstream air |
| ρ_c | = coolant density |
| ρ_m | = mainstream flow density |

Introduction

A CONTINUING trend toward higher gas-turbine inlet temperatures has resulted in higher heat loads on turbine components; therefore, sophisticated cooling techniques must be used to cool the components to maintain the performance requirements. Some turbine blades are cooled by ejecting cooler air from within the blade through discrete holes, which provides a protective film on the surface exposed to the hot gas path. Cooling jet injection can result in higher heat-transfer coefficients downstream of the injection location. However, the heat-transfer rates can still be substantially reduced because of a decreased film-to-wall temperature difference. Many studies have presented heat-transfer measurements on turbine blades with film cooling. Nirmalan and Hylton,¹ Abuaf et al.,² Ames,^{3,4} and Drost and Böls⁵ studied film-cooling heat transfer on film-cooled turbine vanes. Camci and Arts⁶ and Takeishi et al.⁷ studied film-cooling heat transfer on film-cooled turbine blades. Ito et al.⁸ and Haas et al.⁹ studied the effect of coolant density on film-cooling effectiveness on turbine blades under low mainstream turbulence levels.

The effect of unsteady wakes produced by upstream vane trailing edges has a strong effect on rotor blade surface heat-transfer coefficient distributions. Several studies have focused on the effect of unsteady wakes on the downstream blade heat-transfer coefficient distributions without film cooling. They all reported that unsteady wakes enhanced turbine-blade heat transfer and caused earlier and longer laminar-turbulent boundary-layer transition on the suction surface. Few studies have focused on the effect of unsteady wakes on film-cooled turbine blades. Abhari and Epstein¹⁰ conducted heat-transfer experiments on a film-cooled transonic turbine stage in

Presented as Paper 2000-1035 at the AIAA 38th Aerospace Sciences Meeting, Reno, NV, 10–13 January 2000; received 29 June 2000; revision received 22 January 2001; accepted for publication 23 January 2001. Copyright © 2001 by the American Institute of Aeronautics and Astronautics, Inc. All rights reserved.

*Research Assistant, Turbine Heat Transfer Laboratory, Department of Mechanical Engineering; currently Engineer, Heat Transfer Research, Inc., College Station, TX, 77845.

†Marcus Easterling Chair Professor, Turbine Heat Transfer Laboratory, Department of Mechanical Engineering, Associate Fellow AIAA.

‡Research Engineer, Turbomachinery and Propulsion Systems Division.

a short-duration turbine facility. They measured steady and time-resolved, chordwise heat-flux distributions at three spanwise locations. They concluded that film cooling reduces the time-averaged heat transfer by about 60% on the suction surface compared to the uncooled rotor blade. However, the effect is relatively low on the pressure surface. Ou et al.¹¹ and Mehendale et al.¹² simulated unsteady wake conditions over a linear turbine-blade cascade with film cooling. They studied the effects of unsteady wake on a model turbine blade with multiple-row film cooling using air and CO₂ as coolants. They measured heat-transfer coefficients and film-cooling effectiveness at discrete locations using thin foil heating and multiple thermocouples. They concluded that heat-transfer coefficients increase and film-cooling effectiveness values decrease with an increase in unsteady wake strength. Du et al.^{13,14} used a transient liquid crystal technique to measure the detailed heat-transfer coefficient and film effectiveness distributions over a film-cooled turbine blade under the effect of upstream unsteady wakes. They concluded that unsteady wake slightly enhances Nusselt numbers but significantly reduces film-cooling effectiveness on a film-cooled blade surface as compared to a film-cooled blade without unsteady wake. Teng et al.¹⁵ studied unsteady wake effect on film temperature and effectiveness distributions for a gas turbine blade with one row of cylindrical film holes near the suction side gill-hole region. They concluded that unsteady wake reduces film-cooling effectiveness. They also found out that film injection enhances local heat-transfer coefficient, whereas the unsteady wake promotes earlier boundary-layer transition.

To improve the cooling effectiveness and thus increase the life-time of gas turbine blades, an attempt has recently been made to contour the film-hole geometry. Film-cooling holes with a diffuser-shaped expansion at the exit portion of the holes are believed to improve the film-cooling performance on a gas turbine blade. The increased cross-sectional area at the hole exit compared to a standard cylindrical hole leads to reduction of the coolant velocity for a given blowing ratio. The momentum flux of the jet exiting the hole and the penetration of the jet into the mainstream will be reduced accordingly, which results in an increased cooling efficiency. Furthermore, lateral expansion of the hole provides an improved lateral spreading of the jet, which leads to a better coverage of the airfoil in the lateral direction and a higher laterally averaged film-cooling efficiency. A few previous studies have shown that expanding the exit of the cooling hole improves film-cooling performance in comparison to a cylindrical hole. Goldstein et al.¹⁶ reported that overall improvements in adiabatic effectiveness were found for the flat-plate film cooling with laterally expanded holes. Makki and Jekubowski¹⁷ reported that the same improvements were found for forward-expanded holes. Haller and Camus¹⁸ performed aerodynamic loss measurements on a two-dimensional transonic cascade. Holes with a spanwise flare angle of 25 deg were found to offer significant improvements in film-cooling effectiveness without any additional loss penalty. Schmidt et al.¹⁹ and Sen et al.²⁰ compared a cylindrical hole to a forward-expanded hole, both of them having compound angle injection for the flat-plate film cooling. Although the spatially averaged effectiveness for the cylindrical and forward-expanded holes was the same, a larger lateral spreading of the forward-expanded jet was found. Gritsch et al.^{21,22} performed detailed measurements of the flat-plate film-cooling effectiveness and heat-transfer coefficients for single holes with expanded exits. They reported that, compared to the cylindrical holes, the two expanded holes in their study show significantly improved thermal protection of the surface downstream of the ejection location, particularly at the high blowing ratios. Bell et al.²³ studied film cooling from shaped holes on a flat plate and found out that the amount of expansion is critical to the improvement of thermal protection.

All of the preceding studies have proven that film-cooling holes with a diffuser-shaped expansion at the exit portion of the hole have improved film-cooling performance in comparison to cylindrical holes. It is of great interest to understand the effect of the hole shape on turbine-blade heat transfer under turbomachinery flow conditions, that is, consideration of the effect of surface curvature and pressure gradient that exists on a real turbine blade. However, most

of the just-mentioned shape hole film-cooling studies are for flat-plate geometry. There are very few studies present in open literature examining the effects of hole shape on turbine-blade heat transfer under steady and unsteady wake conditions. This study focuses on only one row of film holes near the suction-side gill-hole portion in order to investigate the hole shape effect on the curved blade surface under strong flow acceleration conditions. Film-cooling holes with and without exit expansions are studied and compared under steady and unsteady wake conditions. In the present study a transient liquid crystal method is used to measure the detailed heat-transfer coefficient and film-cooling effectiveness distributions. The high resolution of the liquid crystal technique provides a clear picture of how the heat-transfer coefficient and film-cooling effectiveness distributions vary along the blade surface with different film hole shapes. The results also provide a good database for film-cooling computational model development. This paper focuses on the results of the detailed heat-transfer coefficient distributions. The corresponding results of the detailed film-cooling effectiveness distributions and film-cooling performance are presented in an accompanying paper.²⁴

Experimental Apparatus

Figure 1a shows the schematic of the test section and camera locations. The test apparatus consists of a low-speed wind tunnel with an inlet nozzle, a linear turbine-blade cascade with the test blade in the center, and a suction-type blower. The wind tunnel is designed to accommodate the 107.49-deg turn of the blade cascade. The cascade inlet mean velocity is about 20 m/s. The mean velocity increases 2.5 times from the inlet of the cascade to the exit. The test apparatus was described in detail by Ou et al.¹¹ A spoked-wheel-type wake generator, similar to the one used by Ou et al.,¹¹ simulated the upstream unsteady wake. The wake generator has 32 rods, each 0.63 cm in diameter, to simulate the trailing edge of an upstream vane. The wake Strouhal number is adjusted by controlling the rod rotation

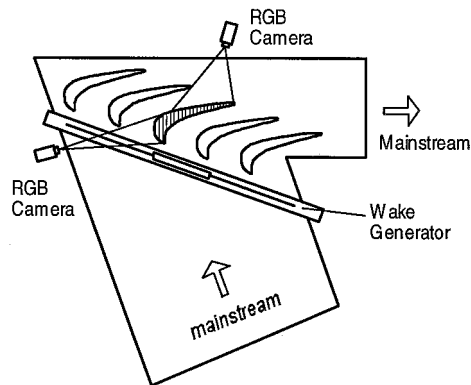


Fig. 1a Five-blade cascade with center blade coated with liquid crystal and viewed by two cameras.

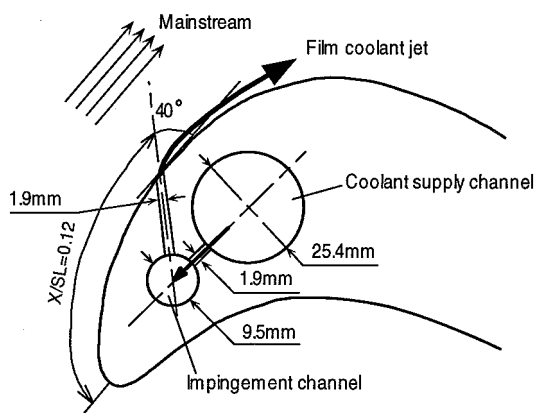


Fig. 1b Two-dimensional view of the film-cooled blade model.

speed N . The error caused by using nonparallel rotating rods with a linear blade cascade was small and was discussed by Ou et al.¹¹ The blade configuration, scaled up five times, produces a velocity distribution typical of an advanced high-pressure turbine-blade row. The cascade has five blades, each with an axial chord length of 17 cm and a radial span of 25.2 cm. The blade spacing is 17.01 cm at the cascade inlet, and the throat-to-bladespan ratio is 0.2. Du et al.¹³ presented the local-to-exit velocity ratio distribution around the blade as well as the instantaneous velocity, ensemble-averaged velocity, and ensemble-averaged turbulence profiles at the cascade inlet under the effect of upstream unsteady wakes. The velocity on the suction side accelerates to about $X/SL = 0.5$ ($V/V_2 = 110\%$) and then decelerates slightly until the exit. In the present study a row of film holes is located near the suction-side gill-hole region $X/SL = 0.12$, where V/V_2 is about 68%, the momentum thickness δ_2 is about 9×10^{-4} m, and the momentum thickness Reynolds number is about 2×10^2 for steady flow. The unsteady wakes are actually velocity deficits caused by the blockage of mainstream flow by the rotating rods. The ensemble-averaged turbulence intensity profiles at the cascade inlet show that intensity could be as high as 20% inside the wake, but the time mean-averaged turbulence intensity is about 10.4%. For cases without unsteady wake effect, that is, without the rotating rods in the mainstream flow, the time mean-averaged turbulence is about 0.7%.

The present film-cooled turbine-blade model is the same as the one used by Teng et al.¹⁵ Figure 1b presents a two-dimensional view of the film-cooled turbine-blade model. There is one cavity used to supply coolant to the row of film holes on the suction side. The film holes, 1.905 mm in diameter and 10.16 mm apart from one another ($P/D = 5.3$), have a radial angle of 90 deg and a tangential angle of 40 deg. The film hole length is 15 mm ($L/D = 7.9$). Flow rate is controlled by a flow meter. The unheated coolant flow is passed through a solenoid-controlled three-way diverter valve before the flow enters the coolant cavity inside the blade. The solenoid-controlled valve is connected to a switch that triggers the coolant flow into the cavity at the instant the transient test is initiated.

The liquid crystal coated surface area is 7.2 cm wide, and the data acquisition area is 2.5 cm wide along the midspan region of the test blade. In heat-transfer measurements the test blade surface is heated uniformly using a heater box.¹⁵ The heater box has the blade shape and is slightly larger than the test blade. The insides of the heater box are instrumented with thin foil heaters and controlled using several variacs to provide a near uniform surface temperature. The heater box is lowered to completely cover the test blade during heating. The heater box is raised completely to expose the test blade to the mainstream during the transient test. The blade surface temperature is monitored using embedded thermocouples during heating. The uniformity of surface temperature with heating is within $\pm 1.2^\circ\text{C}$. An interpolation scheme was used to further reduce the temperature variation in the initial surface temperature to within $\pm 0.2^\circ\text{C}$. In the present study the blade surface is heated to a temperature above liquid crystal blue color (37.2°C). The mainstream air is turned on by starting the suction-type blower. When the blower reaches the stable test flow conditions, the heater box is raised to expose the hot blade to the room temperature mainstream air within 0.1 s. When the heater box completely clears the blade height, the liquid crystal data acquisition system is automatically triggered. The liquid crystal color change time is measured using a high-precision image-processing system. The transient tests last about 60–90 s in average. The system consists of two cameras individually connected to a color frame grabber board in the personal computer and a monitor. Software is used to measure the time of color change of liquid crystals. During one test, only one camera is operational. Hence, we require two different runs with two different camera locations to measure one set of data on the suction side for a particular condition. Details on the image-processing system were presented by Teng et al.¹⁵ The image-processing system consists of an RGB camera, monitor, and a personal computer with color frame grabber board.

Figure 2 presents the three types of hole geometries studied: cylindrical hole, fan-shaped hole, and laidback fan-shaped hole. The hole geometries are similar to those used by Gritsch et al.²¹ They have

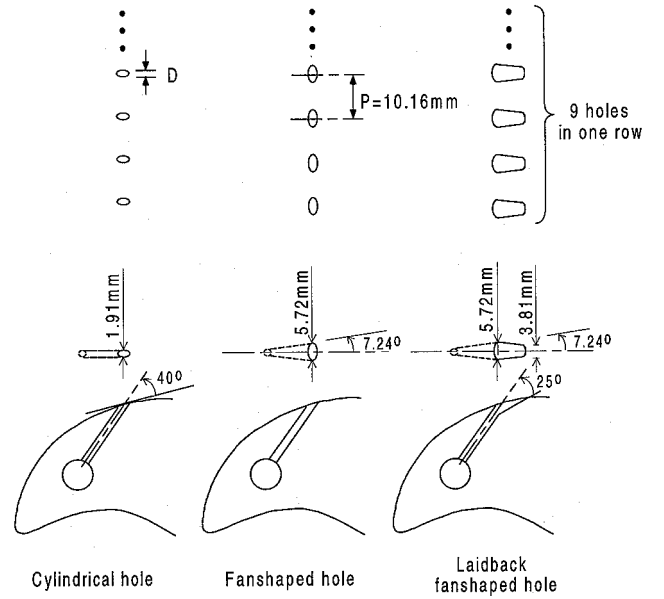


Fig. 2 Film-cooling hole geometries.

shown that, in flat-plate geometry, expanded holes show significantly improved thermal protection of the surface downstream of the ejection location as compared to the cylindrical hole. In the present study a row of nine holes of each shape located near the blade suction-side gill-hole region ($X/SL = 0.12$) has been employed. The diameter of the cylindrical hole D and diameter of the cylindrical inlet section of the expanded hole is 1.91 mm. For all geometries the inclination angle is 40 deg, the pitch-to-diameter ratio is $P/D = 5.3$, and the length-to-diameter ratio L/D is 7.9. The lateral expansion angle of both expanded holes is 7.24 deg. The exit forward expansion angle of the laidback fan-shaped hole is 25 deg. For the fan-shaped and laidback fan-shaped hole the calculation of the blowing ratio was based on the inlet cross-sectional area of these holes, that is, the same as the cylindrical hole. In this study this means that the same blowing ratio provides the same amount of coolant ejected under the same mainstream condition. Thus, the blowing ratio of the shaped holes can be directly compared to those of the cylindrical hole, which makes it more convenient to evaluate the effect of the hole exit shape.

Data Analysis

A transient liquid crystal technique was used to measure the detailed heat-transfer coefficients and film-cooling effectiveness on the blade suction surface. The technique is similar to the one described by Teng et al.¹⁵ A one-dimensional transient conduction model into a semi-infinite solid with convective boundary condition is assumed. The solution for surface temperature is obtained as

$$\frac{T_w - T_i}{T_m - T_i} = \left[1 - \exp\left(\frac{h^2 \alpha t}{k^2}\right) \operatorname{erfc}\left(\frac{h \sqrt{\alpha t}}{k}\right) \right] \quad (1)$$

where T_w is the wall temperature when liquid crystals change to red from green (32.7°C) at time t . The heat transfer coefficient is obtained from Eq. 1. The preceding equation is solved at each point on the blade surface (16,600 points) to obtain the detailed heat-transfer coefficient distributions.

The average uncertainty in heat-transfer coefficient measurement was estimated to be $\pm 6.5\%$. The individual uncertainties in the measurement of the time of color change ($\Delta t = \pm 5\%$), the mainstream temperature ($\Delta T_m = \pm 1.3\%$), the initial temperature ($\Delta T_i = \pm 0.6\%$), the color change temperature ($\Delta T_w = \pm 3\%$), and the wall material properties ($\Delta \alpha/k^2 = \pm 2\%$) are included in the calculation of the overall uncertainty in the measurement. The uncertainty in the immediate vicinity of the hole (less than 1 diameter around the hole) could be higher as a result of invalidation of the one-dimensional semi-infinite model assumption.

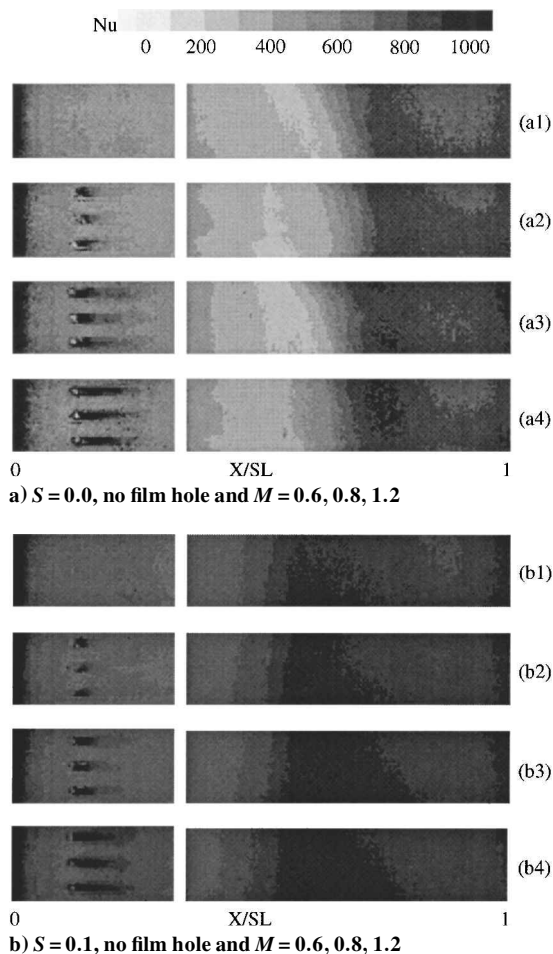


Fig. 3 Detailed Nusselt-number distributions of cylindrical holes for cases at different blowing ratios, with and without wake effect.

Results and Discussion

Experiments were performed at a cascade exit Reynolds number of 5.3×10^5 . The corresponding flow velocity at the cascade exit was 50 m/s. Air as coolant was tested at blowing ratios of 0.4, 0.6, 0.8, and 1.2 for the no-rod, no-wake cases ($S = 0$, $\bar{T}u = 0.7\%$) and cases with wake ($S = 0.1$, $\bar{T}u = 10.4\%$).

Detailed Heat-Transfer Coefficient Distributions

Figures 3–5 present the detailed heat-transfer coefficient distributions for cylindrical, fan-shaped, and laidback fan-shaped cooling holes, respectively. Figures labeled (a1–a5) are for the cases without wake effect and figures labeled (b1–b5) are for the cases with wake effect. Additionally, (a1) and (b1) are for the cases without film holes, and the others in each group have blowing ratios ranging from 0.4 to 1.2.

For a no film-hole blade without wake effect case (a1), the Nusselt numbers drop rapidly from the leading edge to about $X/SL = 0.5$ on the suction surface, and then increase again because of the boundary-layer transition to turbulent flow. The Nusselt numbers also decrease along the streamwise direction for a no film-hole blade with wake effect (case b1), but the boundary-layer transition occurs much earlier ($X/SL = 0.25$) for this case than for case a1. Also, the Nusselt numbers for case (b1) are higher than case (a1) before the transition begins.

Film injection through cylindrical holes (Fig. 3) causes the Nusselt numbers at locations immediately downstream of the film holes to increase significantly as a result of the mainstream and coolant jet interaction. Traces of high Nusselt numbers are formed immediately downstream of the film holes. The higher the blowing ratio, that is, the more mixing between the mainstream and the coolant jet, the longer this trace of highly increased Nusselt num-

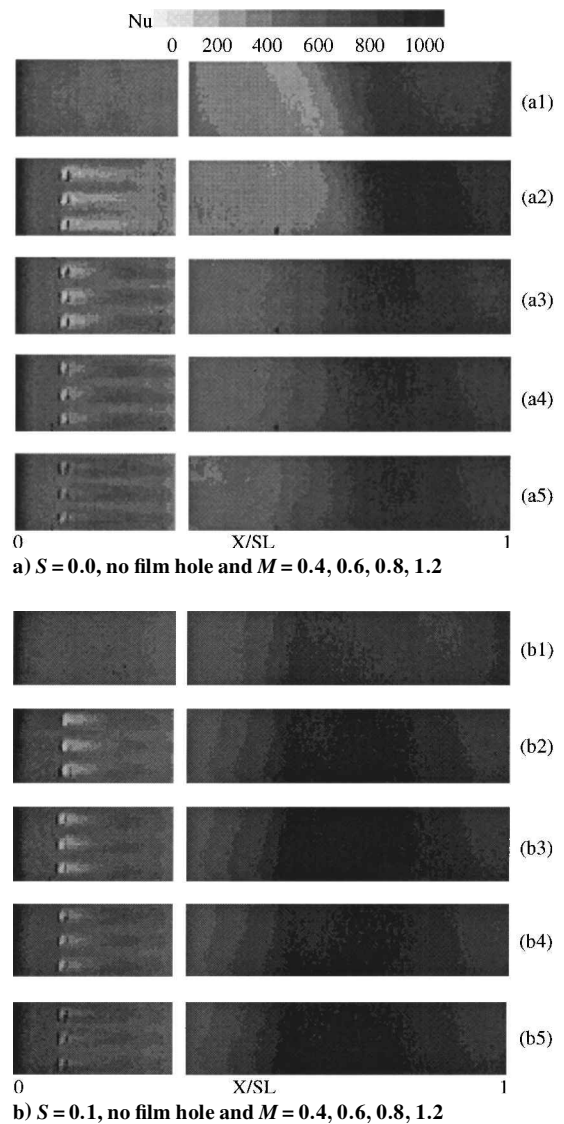


Fig. 4 Detailed Nusselt-number distributions of fan-shaped holes for cases at different blowing ratios, with and without wake effect.

bers. The film injection disturbs the boundary layer, which causes transition to occur slightly earlier for cases (a2–a4) than case (a1). As soon as the boundary-layer transition begins, the Nusselt numbers increase at about the same rate as case (a1) and keep increasing further down the blade before beginning to decrease. The same is true for the cases with both film cooling and unsteady wake effect, as seen by comparing cases (b2–b4) with case (b1). However, notice that, with or without film cooling, the addition of unsteady wake has caused the boundary-layer transition to occur significantly earlier than the cases without unsteady wake. This is because unsteady wake interacts with the boundary layer; thus causing an earlier boundary-layer transition and enhancing the surface heat transfer. Also, the cases with wake effect show that streaks of high Nusselt numbers immediately downstream of the film holes are a little shorter when compared to the cases without wake effect. This is caused by the unsteady wake, which causes the cooling jet to dilute faster along the streamwise direction than in the cases without unsteady wake.

For film injection through fan-shaped holes (Fig. 4), the Nusselt numbers immediately downstream of the film ejection location are significantly reduced when compared with the no film-hole case (a1). Traces of low Nusselt number are formed immediately downstream of the fan-shaped film holes. This is because film injection through the fan-shaped holes has a lower momentum compared with a cylindrical hole case with the same blowing ratio. The lower momentum coolant jets from the fan-shaped holes tend to stay closer

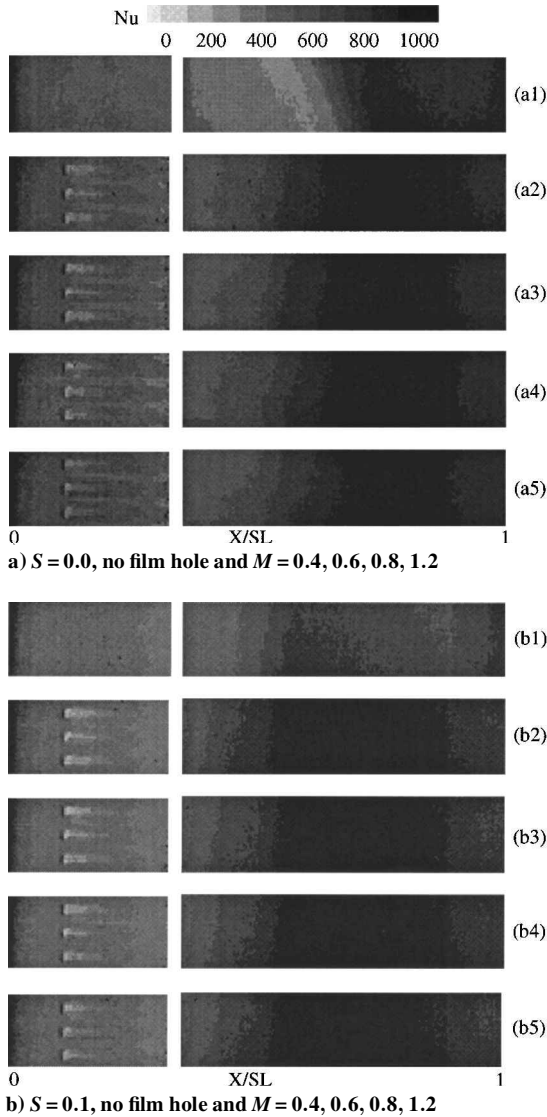


Fig. 5 Detailed Nusselt-number distributions of laidback fan-shaped holes for cases at different blowing ratios, with and without wake effect.

to the blade surface, which reduces interaction (mixing) with the mainstream. Nusselt numbers downstream of the injection location increase along the streamwise direction as the mainstream begins to interact with the coolant jet. The Nusselt numbers also increase with the increase of blowing ratio as a result of the increased jet-to-mainstream interaction. Similar to the cylindrical hole cases, the boundary-layer transition for fan-shaped holes (a2–a5) occurs slightly earlier than the no film-hole case (a1) because of the film injection. As soon as the boundary-layer transition begins, the Nusselt numbers increase at a slower rate than the no film-hole case (a1) and keep increasing further down the blade before beginning to decrease again. The same is true for cases with both film cooling and unsteady wake effect, as seen by comparing cases (b2–b5) with case (b1). The addition of the unsteady wake effect causes boundary-layer transition to occur significantly earlier than in the cases without unsteady wake. Also, for cases with wake effect, the streaks of low Nusselt region immediately downstream of the film holes are reduced compared with cases without wake effect, which is caused by the interaction between the unsteady wake and the boundary layer.

Traces of low Nusselt number form immediately downstream of the film holes for cases of laidback fan-shaped holes (Fig. 5). The Nusselt numbers are slightly higher, and the boundary-layer transition occurs slightly earlier in comparison with their corresponding cases for fan-shaped holes. The wide traces of low Nusselt number immediately downstream of the fan-shaped and laidback fan-shaped

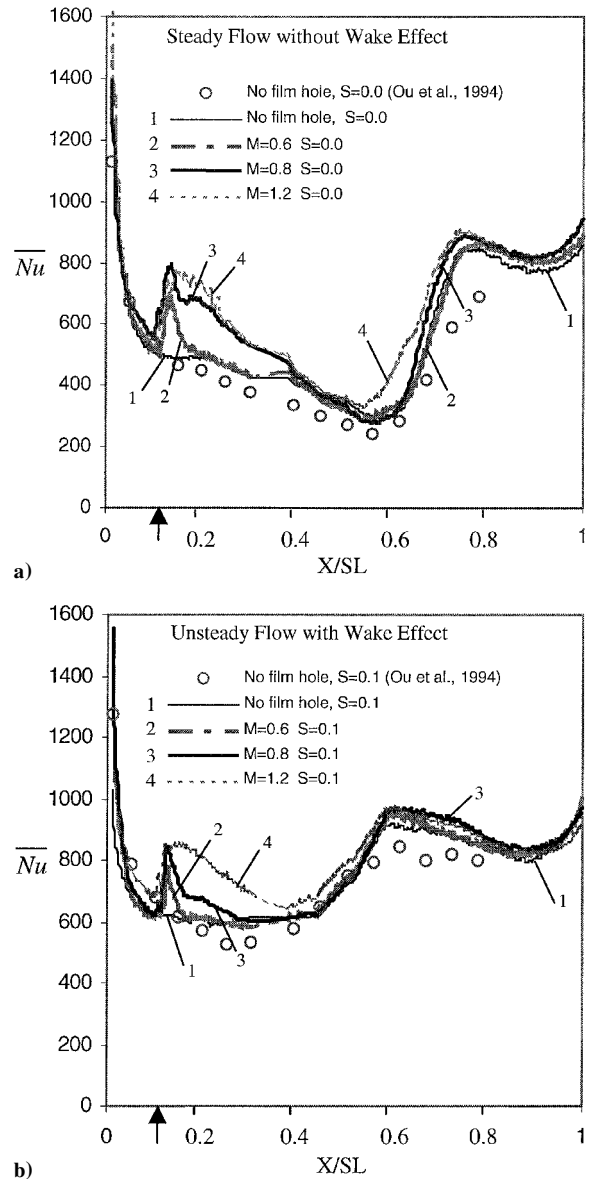


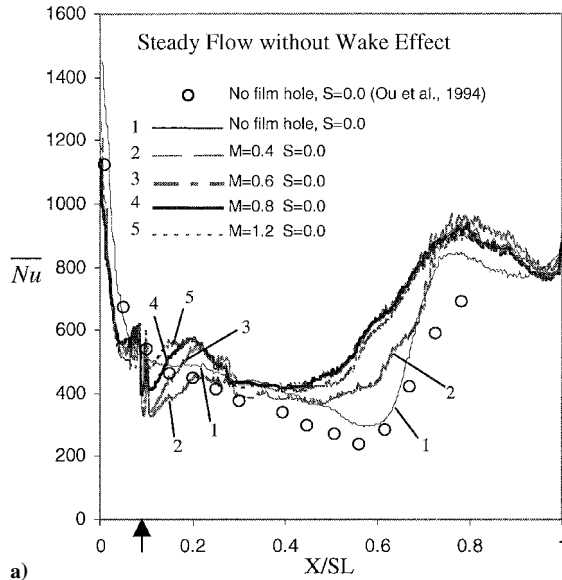
Fig. 6 Spanwise-averaged Nusselt-number distributions of cylindrical holes for a) steady flow, $S = 0.0$ and b) unsteady flow with wake effect, $S = 0.1$.

film holes, especially for the cases without wake effect, indicate a low heat-transfer rate between the blade surface and the cooling jet, and thus a much improved thermal protection in comparison to the standard cylindrical hole film cooling. However, film injection through fan-shaped and laidback fan-shaped holes induce earlier boundary-layer transition compared with cylindrical holes. The Nusselt number after boundary-layer transition is also higher for fan-shaped and laidback fan-shaped hole injection.

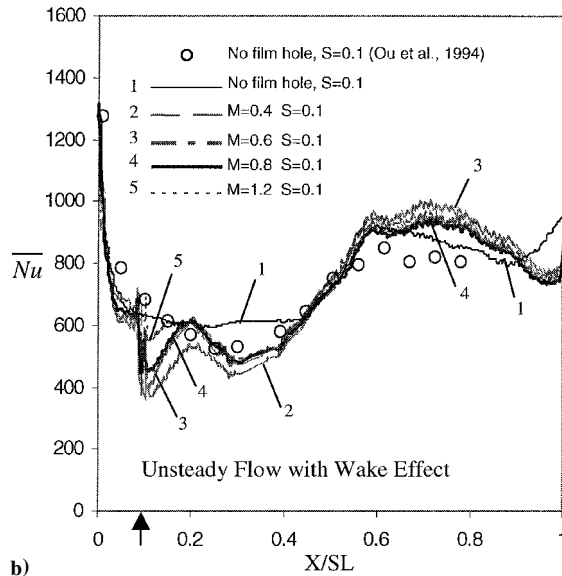
Spanwise-Averaged Heat-Transfer Coefficient Distributions

Figure 6–8 present the spanwise-averaged Nusselt number distributions of cylindrical, fan-shaped and laidback fan-shaped holes for 1) steady flow and 2) unsteady flow with wake effect. The small arrows on the horizontal coordinate indicate the location of film injection ($X/SL = 0.12$). The results for the no film-hole blade with and without wake effect agree with those for the same cases from Ou et al.,¹¹ who used the thin-foil-thermocouple technique to study the heat-transfer coefficient over the same turbine-blade model.

Figure 6 presents the spanwise-averaged Nusselt number distributions for film injection through cylindrical holes. The spanwise-averaged Nusselt number shows a peak increase right downstream of the jet ejection location. It then decreases along the streamwise



a)

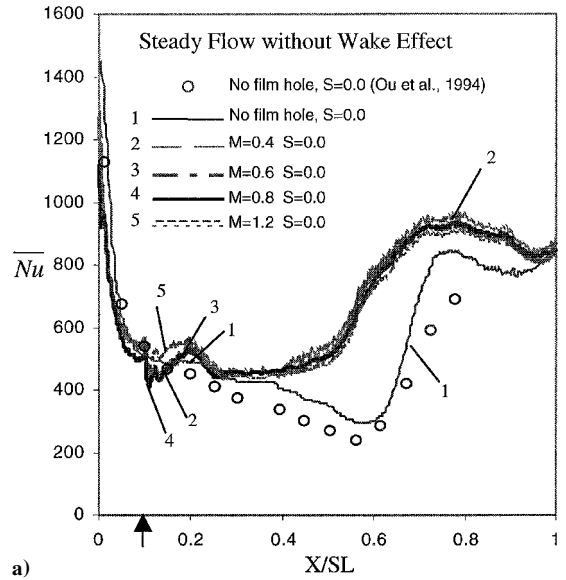


b)

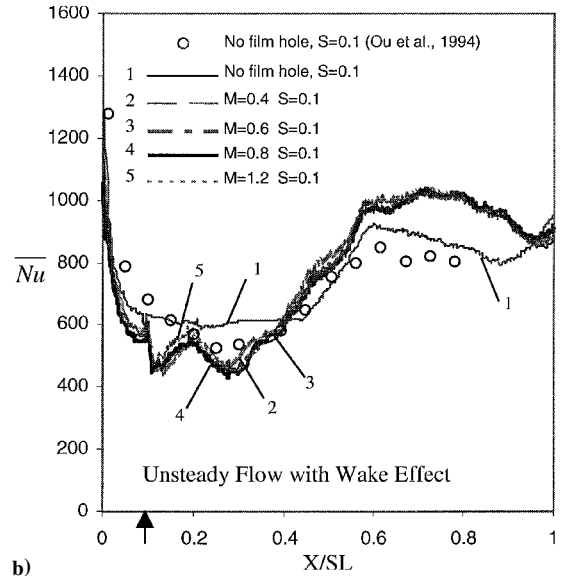
Fig. 7 Spanwise-averaged Nusselt-number distributions of fan-shaped holes for a) steady flow, $S = 0.0$ and b) unsteady flow with wake effect, $S = 0.1$.

direction until it reaches the boundary-layer transition location, where it begins to increase again to reach its second peak value. The second peak value is higher than the first one. For the cases with wake effect, however, the spanwise-averaged Nusselt numbers do not drop as low as the cases without wake effect before they begin to increase again as a result of a much earlier boundary-layer transition. Figure 6 shows that the Nusselt numbers downstream of the injection location increase with blowing ratio. This is because an increased blowing ratio causes more interaction (mixing) between the coolant jet and the mainstream and, thus, increase the heat-transfer coefficients. For a high blowing ratio of 1.2, the Nusselt numbers downstream of the injection location can increase up to 60%. The spanwise-averaged Nusselt numbers do not show much difference between different blowing ratios after the boundary-layer transition. The addition of the unsteady wake effect promotes earlier boundary-layer transition for all blowing ratios. In comparison to cases without wake effect, the spanwise-averaged Nusselt numbers do not drop much before the boundary-layer transition occurs. The blowing ratio effect is very small compared with the effect of unsteady wake as far as the boundary-layer transition location is concerned.

Figure 7 shows that the spanwise-averaged Nusselt numbers also increase with the increase of blowing ratio for film injection through



a)



b)

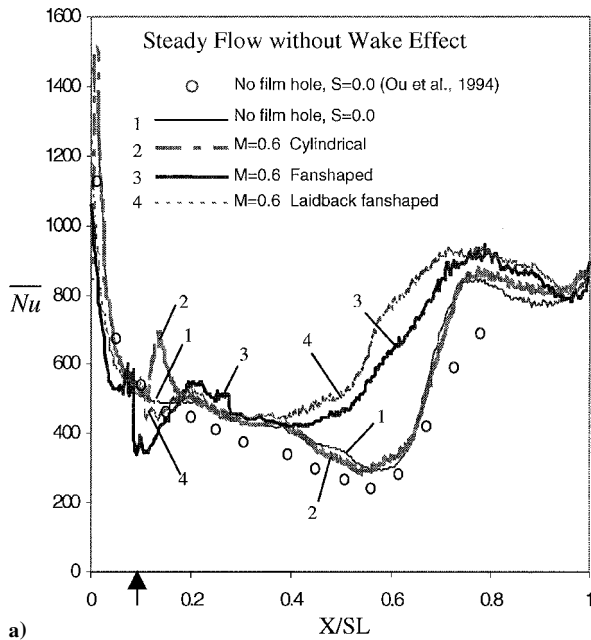
Fig. 8 Spanwise-averaged Nusselt-number distributions of laidback fan-shaped holes for a) steady flow, $S = 0.0$ and b) unsteady flow with wake effect, $S = 0.1$.

fan-shaped holes. However, the spanwise-averaged Nusselt numbers immediately downstream of the film ejection location are lower than that of the no film-hole case. The Nusselt numbers downstream of the injection location can decrease up to 40% for a low blowing ratio of 0.4. Boundary-layer transition occurs earlier as the blowing ratio increases. With the addition of unsteady wake, boundary-layer transition occurs even earlier, but distinguishes the blowing ratio effect on boundary-layer transition.

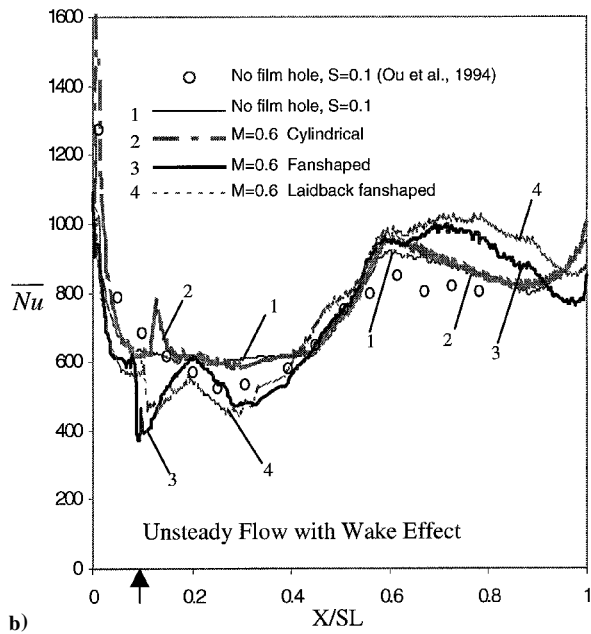
Film injection through laidback fan-shaped holes (Fig. 8) has spanwise-averaged Nusselt-number distributions that are insensitive to blowing ratios, either under steady or unsteady flow conditions. At the locations immediately downstream of the film injection, the spanwise-averaged Nusselt numbers are slightly lower than that of no film-hole case when there is no wake effect, whereas they are much lower (up to 25–30%) than when there is wake effect. Unsteady wake effect also promotes earlier boundary transition for film injection through laidback fan-shaped holes.

Effect of Hole Shape

Figure 9 presents the effect of hole shape on spanwise-averaged Nusselt-number distributions for cases at a low blowing ratio of $M = 0.6$. For film injection through fan-shaped and laidback fan-shaped holes, the spanwise-averaged Nusselt numbers immediately



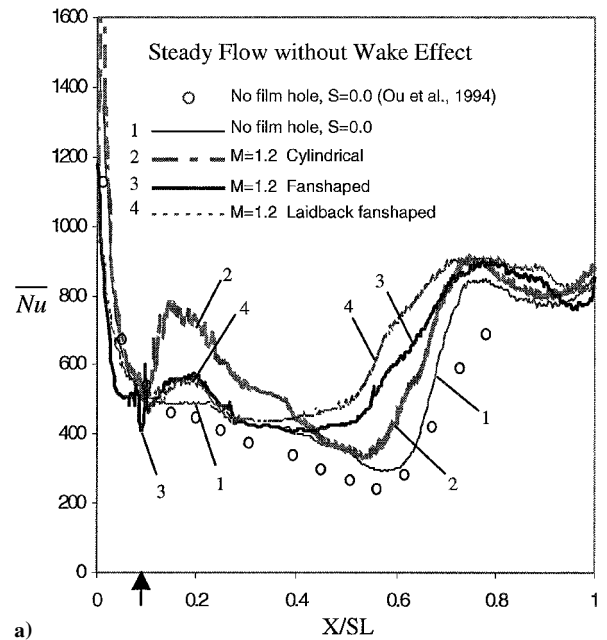
a)



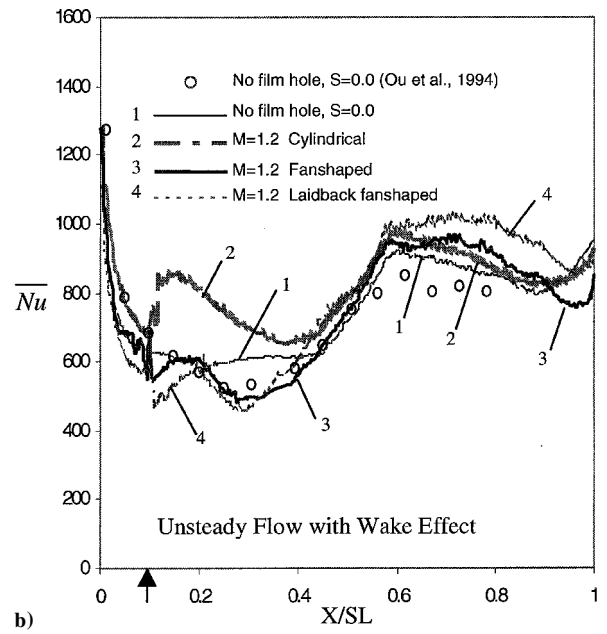
b)

Fig. 9 Effect of hole shape on spanwise-averaged Nusselt-number distributions for $M = 0.6$: a) steady flow, $S = 0.0$ and b) unsteady flow with wake effect, $S = 0.1$.

downstream of the film ejection location are much lower than that for the cylindrical hole case. This implies that, for fan-shaped and laidback fan-shaped hole injection, the coolant jet with reduced momentum tends to attach to the blade surface and thus reduces the interaction with mainstream at locations immediately downstream of the film injection. However, the low-momentum jet may stay in but disturb the laminar boundary layer along the blade surface. This causes an earlier boundary-layer transition for both fan-shaped hole injections in comparison with the cylindrical hole injection. Because of earlier boundary-layer transition, the spanwise-averaged Nusselt numbers of both fan-shaped and laidback fan-shaped holes are much higher than that of the cylindrical hole case in the latter part of the blade surface. The addition of unsteady wake has led to an increased Nusselt-number difference in the front part of the blade surface: the region downstream of injection where the spanwise-averaged Nusselt numbers of fan-shaped and laidback fan-shaped holes are less than that of the cylindrical hole case is more than doubled in the streamwise direction. However, the boundary-layer transition



a)



b)

Fig. 10 Effect of hole shape on spanwise-averaged Nusselt-number distributions for $M = 1.2$: a) steady flow, $S = 0.0$ and b) unsteady flow with wake effect, $S = 0.1$.

location is almost the same for the three types of film hole injection and the no film-hole case when there is unsteady wake effect.

Figure 10 presents the effect of hole shape on spanwise-averaged Nusselt-number distributions for cases with a high blowing ratio of $M = 1.2$. The general trend is almost the same as the cases with $M = 0.6$. For the cases under steady flow condition, the spanwise-averaged Nusselt number is higher than that of no film-hole case for all three kinds of holes. Film injection through cylindrical holes produces the highest spanwise-averaged Nusselt numbers in the region immediately downstream of the film injection location, whereas fan-shaped and laidback fan-shaped hole injection have higher spanwise-averaged Nusselt numbers at the latter part of the blade surface. With the addition of unsteady wake, the hole effect is intensified at the front part of the blade. In the region immediately downstream of film injection, the spanwise-averaged Nusselt numbers for fan-shaped and laidback fan-shaped hole injection are much lower than that of cylindrical hole injection. The differences of the spanwise-averaged Nusselt numbers for different hole injection are

reduced at the rear part of the blade surface. The boundary-layer transition location is almost the same for the three types of film hole and the no film-hole case when there is an unsteady wake effect.

Conclusions

Detailed measurements of heat-transfer coefficients on a gas turbine blade are presented. The film-hole geometries studied include standard cylindrical holes and holes with a diffuser-shaped exit portion (i.e., fan-shaped holes and laidback fan-shaped holes). The results show that the cooling hole shape has an important impact on the heat-transfer coefficient distribution. The conclusions based on the experimental results are the following:

1) For film injection through cylindrical holes, the Nusselt numbers downstream of the injection location increase with an increase in blowing ratio. The Nusselt numbers downstream of the injection location can increase up to 60% for a high blowing ratio of 1.2 as compared with no film-hole case. Unsteady wake promotes earlier boundary-layer transition regardless of the influences of the blowing ratio.

2) For film injection through fan-shaped holes, the Nusselt numbers downstream of the injection location increase with an increase in blowing ratio; however, they are lower than that of the no film-hole case. The Nusselt numbers downstream of the injection location can decrease up to 40% for a low blowing ratio of 0.4. However, fan-shaped hole injection promotes earlier boundary-layer transition as the blowing ratio increases. Unsteady wake causes earlier boundary-layer transition regardless of the blowing ratio effect.

3) The Nusselt numbers are insensitive to blowing ratios for film injection through laidback fan-shaped holes. Unsteady wake again causes an even earlier boundary-layer transition regardless of the blowing ratio effect.

4) For steady flow, when compared with cylindrical holes, both fan-shaped and laidback fan-shaped holes have much lower Nusselt numbers immediately downstream of the film injection location. However, they cause higher heat-transfer coefficients in the latter part of the blade surface as a result of earlier boundary-layer transition.

5) For unsteady flow, when compared with cylindrical holes, both fan-shaped and laidback fan-shaped holes also have much lower Nusselt numbers immediately downstream of the film injection location. They have almost the same boundary-layer transition location as the cylindrical hole case, yet their Nusselt numbers are higher after transition into the turbulent region.

Acknowledgments

This paper was prepared with the support of the NASA Lewis Research Center under Grant Number NAG3-1656. The NASA technical team is Philip E. Poinssatte and Raymond Gaugler. Their support is greatly appreciated.

References

- ¹Nirmalan, V., and Hylton, L., "An Experimental Study of Turbine Vane Heat Transfer with Leading Edge and Downstream Film Cooling," *Journal of Turbomachinery*, Vol. 112, No. 3, 1990, pp. 477-487.
- ²Abuaf, N., Bunker, R., and Lee, C. P., "Heat Transfer and Film Cooling Effectiveness in a Linear Airfoil Cascade," American Society of Mechanical Engineers, Paper 95-GT-3, June 1995.
- ³Ames, F. E., "Aspects of Vane Film Cooling with High Turbulence: Part I—Heat Transfer," American Society of Mechanical Engineers, Paper 97-GT-239, June 1997.
- ⁴Ames, F. E., "Aspects of Vane Film Cooling with High Turbulence: Part II—Adiabatic Effectiveness," American Society of Mechanical Engineers, Paper 97-GT-240, June 1997.
- ⁵Drost, U., and Böls, A., "Investigation of Detailed Film Cooling Effectiveness and Heat Transfer Distributions on a Gas Turbine Airfoil," American Society of Mechanical Engineers, Paper 98-GT-20, June 1998.
- ⁶Camci, C., and Arts, T., "An Experimental Convective Heat Transfer Investigation Around a Film-Cooled Gas Turbine Blade," *Journal of Turbomachinery*, Vol. 112, No. 3, 1990, pp. 497-503.
- ⁷Takeishi, K., Aoki, A., Sato, T., and Tsukagoshi, K., "Film Cooling on a Gas Turbine Rotor Blade," *Journal of Turbomachinery*, Vol. 114, No. 4, 1992, pp. 828-834.
- ⁸Ito, S., Goldstein, R. J., and Eckert, E. R. G., "Film Cooling of a Gas Turbine Blade," *Journal of Engineering for Power*, Vol. 100, No. 3, 1978, pp. 476-481.
- ⁹Haas, W., Rodi, W., and Schönung, B., "The Influence of Density Difference Between Hot and Coolant Gas on Film Cooling by a Row of Holes: Predictions and Experiments," *Journal of Turbomachinery*, Vol. 114, No. 4, 1992, pp. 747-755.
- ¹⁰Abhari, R. S., and Epstein, A. H., "An Experimental Study of Film Cooling in a Rotating Transonic Turbine," *Journal of Turbomachinery*, Vol. 116, No. 1, 1994, pp. 63-70.
- ¹¹Ou, S., Han, J. C., Mehendale, A. G., and Lee, C. P., "Unsteady Wake over a Linear Turbine Blade Cascade with Air and CO₂ Film Injection: Part I—Effect on Heat Transfer Coefficients," *Journal of Turbomachinery*, Vol. 116, No. 4, 1994, pp. 721-729.
- ¹²Mehendale, A. B., Han, J. C., Ou, S., and Lee, C. P., "Unsteady Wake over a Linear Turbine Blade Cascade with Air and CO₂ Film Injection: Part II—Effect on Film Effectiveness and Heat Transfer Distributions," *Journal of Turbomachinery*, Vol. 116, No. 4, 1994, pp. 730-737.
- ¹³Du, H., Han, J. C., and Ekkard, S. V., "Effect of Unsteady Wake on Detailed Heat Transfer Coefficient and Film Effectiveness Distributions for a Gas Turbine Blade," *Journal of Turbomachinery*, Vol. 120, No. 4, 1998, pp. 808-817.
- ¹⁴Du, H., Ekkad, S. V., and Han, J. C., "Effect of Unsteady Wake with Trailing Edge Coolant Ejection on Film Cooling Performance for a Gas Turbine Blade," *Journal of Turbomachinery*, Vol. 121, No. 3, 1999, pp. 448-455.
- ¹⁵Teng, S., Sohn, D. K., and Han, J. C., "Unsteady Wake Effect on Film Temperature and Effectiveness Distributions for a Gas Turbine Blade," *Journal of Turbomachinery*, Vol. 122, No. 2, 2000, pp. 340-347.
- ¹⁶Goldstein, R., Eckert, E., and Burggraf, F., "Effects of Hole Geometry and Density on Three-Dimensional Film Cooling," *International Journal of Heat and Mass Transfer*, Vol. 17, No. 4, 1974, pp. 595-607.
- ¹⁷Makki, Y., and Jekubowski, G., "An Experimental Study of Film Cooling from Diffused Trapezoidal Shaped Holes," AIAA Paper 86-1326, June 1986.
- ¹⁸Haller, B., and Camus, J., "Aerodynamic Loss Penalty Produced by Film Cooling Transonic Turbine Blades," American Society of Mechanical Engineers, Paper 83-GT-77, March 1983.
- ¹⁹Schmidt, D., Sen, B., and Bogard, D., "Film Cooling with Compound Angle Holes: Adiabatic Effectiveness," American Society of Mechanical Engineers, Paper 94-GT-312, June 1994.
- ²⁰Sen, B., Schmidt, D. L., and Bogard, D. G., "Film Cooling with Compound Angle Holes: Heat Transfer," American Society of Mechanical Engineers, Paper 94-GT-311, June 1994.
- ²¹Gritsch, M., Schulz, A., and Wittig, S., "Adiabatic Wall Effectiveness Measurements of Film-Cooling Holes with Expanded Exits," American Society of Mechanical Engineers, Paper 97-GT-164, June 1997.
- ²²Gritsch, M., Schulz, A., and Wittig, S., "Heat Transfer Coefficient Measurements of Film-Cooling Holes with Expanded Exits," American Society of Mechanical Engineers, Paper 98-GT-28, June 1998.
- ²³Bell, C. M., Hamakawa, H., and Ligrani, P. M., "Film Cooling from Shaped Holes," *Journal of Heat Transfer*, Vol. 122, No. 2, 2000, pp. 224-232.
- ²⁴Teng, S., Han, J. C., and Poinssatte, P. E., "Effect of Film-Hole Shape on Turbine Blade Film Cooling Performance," *Journal of Thermophysics and Heat Transfer*, Vol. 15, No. 3, 2001, pp. 257-265.